Preparation of WS_2 Nanosheets from Lithium Intercalation for Hydrogen Evolution

Yu-Shun Chen[1, 2], Chia-Wei Chang[1], Kuan-Bo Lin[1, 2], Min-Hsiung Hon[1], Chao-Cheng Kaun[2*] and Yen-Hsun Su[1*]

[1]*Department of Materials Science and Engineering, National Cheng Kung University, No. 1, University Road, Tainan City 701, Taiwan, ROC*
[2]*Research Center for Applied Sciences, Academia Sinica, 128 Sec. 2, Academia Road, Nankang, Taipei 11529, Taiwan, ROC*

[*]Corresponding author

DOI: 10.5185/amlett.2018.1923
www.vbripress.com/aml

Abstract

In this content, the few-layered 1T-WS_2 nanosheets were prepared by chemical exfoliation and applied to study hydrogen evolution reaction. Lithium were introduced from n-butyllithium in hexane solution and showed intercalation into the bulk WS_2 powder to form the Li_xWS_2 compound in a teflon lined autoclave at a temperature of 100^0C for 5 hours. Different concentration of n-butyllithium solution were used with the intention of observing the as-prepared nanosheet properties and the influence on the hydrogen evolution reaction. After the Li_xWS_2 powder reacted with DI-water and underwent ultrasonic treatment, the few-layered 1T-WS_2 nanosheets were obtained. The size of the as-preapared nanosheets was in the scale of several hundred nanometers. The layer number of the sheets can be observed and determined as about the range of three to six layers. Furthermore, the measurements of UV-vis, TEM (Transmission Electron Microscope), AFM (Atomic Force Microscope) and hydrogen evolution reaction were carried out. In this report, the 1T-WS_2 nanosheets show excellent catalytic activity for hydrogen evolution reaction. This indicates that 1T-WS_2 nanosheets are promising in sustainable production of hydrogen fuel and increasing the efficiency of hydrogen production. Copyright © 2018 VBRI Press.

Keywords: Lithium intercalation, WS_2, nanosheet, hydrogen evolution reaction.

Introduction

Nowadays, two dimensional materials have received a lot of attention. The most well-known 2D material is graphene [1-3]. Recently, the two dimensional transition metal dichalcogenides such as MoS_2 monolayer and WS_2 monolayer, have caught a lot of attention. Layered transition metal dichalcogenides (LTMDs) are the most promising two dimensional materials because of their multiple applications in catalysis, light emitting diodes and phototransistors [4-7]. However, the semiconducting 2H-WS_2 nanosheets only show catalytically active along edges and catalytically inert in the basal planes [8]. Recent reports show that the catalytic performance of semiconducting 2H-WS_2 can be significantly improved by phase conversion to metallic 1T-WS_2 [9-11]. Lithium intercalation is a useful way of chemical exfoliation method to prepare a large-scale 1T-WS_2 nanosheets. By using the n-butyllithium, the lithium ion is inserted into the layered structures of bulk WS_2 [12]. The Li_xWS_2 compound is exfoliated in water and undergo ultrasonic treatment.

Recently, global warming has been resulting in steep rise of temperature, related to the excess usage of fossil fuel with the large emission of CO_2. It is in urgent need of finding other resources to replace fossil fuel. Hydrogen fuel is a suitable resource because of its characteristic of high energy density and clean by-product (water) after combustion [13]. Nowadays, Platinum is the most efficient catalyst for hydrogen evolution reaction [14]. However, Platinum is still very expensive, so that it is difficult to be widely used. Here, we report that WS_2 nanosheets have a potential to be a great candidate of catalyst for hydrogen evolution reaction. With the help of this novel material, the problems of environmental pollution and energy shortage can be significantly improved.

Experimental

Preparation of WS_2 nanosheets

Tungsten disulphide nanosheets were prepared by the reaction of lithium intercalated WS_2 with distilled and deionized water. Bulk WS_2 powder (0.62 g, Sigma-Aldrich) was mixed with three different concentrations of n-butyllithium (Rockwood) in hexane – 0.33 M, 0.50 M and 0.67 M. Then the mixture was heated at 100^0C in a teflon lined autoclave for 5 hour. After 5 hours, the lithium intercalated WS_2 was washed with 50 ml of hexane twice to remove the excess n-butyllithium, followed by exfoliation in 40 ml of distilled and deionized water under ultrasonication for 50 min. Equal volume of ethanol was added into the WS_2 nanosheets solution and centrifuged at

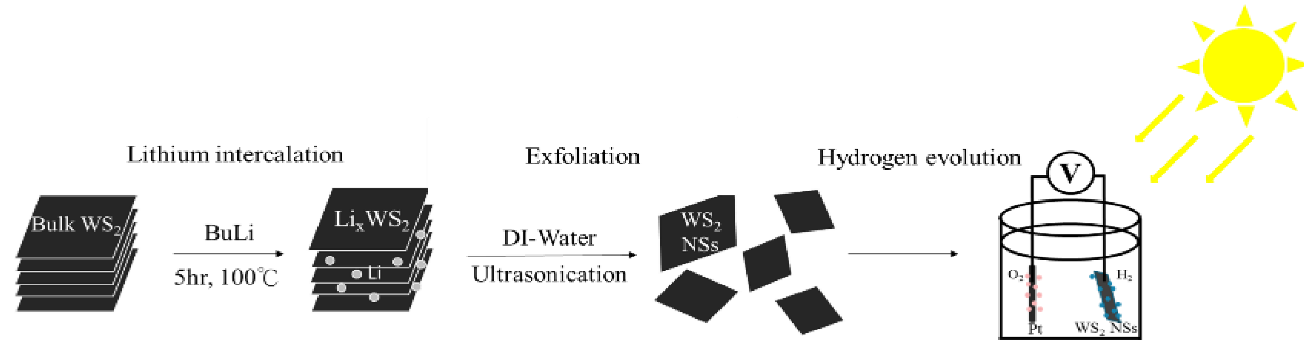

Fig. 1. The illustration of WS_2 nanosheets preparation and water splitting reaction.

6,000 rpm for 20 min. The unexfoliated materials in the bottom of tube were removed and repeated the centrifugation procedure. The supernatant was then centrifuged at 14,000 with 95 % of ethanol solution several times to remove lithium cations. At least, the WS_2 nanosheets were dispersed in ethanol.

Electrochemistry measurement of WS_2 nanosheets

The WS_2 nanosheets were dispersed in ethanol with 3 % of PEDOT:PSS in H_2O and were transferred on the ITO substrate. The electrolyte was prepared by mixing 0.2 M $KHCO_3$ water solution with methanol (1:1 in volume).The efficiency (η) of photoelectrochemical water splitting was evaluated according to the following equation [15]:

$$\eta(\%)=\frac{(1.229-|Vbias|)\times I}{Pt}\times 100\%,$$

where η is the photoelectric conversion efficiency, I is the photocurrent density at V bias, Pt is the intensity of incident solar light. The illustration of the experiment is show in the **Fig. 1.**

Results and discussion

Crystalline Structure and Morphology Characteristic of WS_2 nanosheets

From the SEM image in **Fig. 2,** the bulk WS_2 lateral size is 2-5 µm. In contrast with substrate, the bulk WS_2 is multilayer stacking together. By the method of solvothermal, the lithium is intercalated into the interlayer of bulk WS_2 and the van der Waals force between each layer is decreased [16]. The interlayer distance is then expanded by the lithium intercalation. After the insertion of lithium, the Li_xWS_2 compound is reacted with H_2O to generate hydrogen gas under ultrasonication[17]. The exfoliation is enhanced by the hydrogen gas and ultrasonication. The TEM image of three different concentration of n-butyllithium (0.33 M, 0.50 M and 0.67 M) is shown in **Fig. 3.** From the **Fig. 3,** the WS_2 nanosheets are almost transparent which indicates that the WS_2 nanosheets contain few layer [18]. The lateral sizes of WS_2 nanosheets are about 100-200 nm. The thickness of WS_2 nanosheets were determined by AFM. The height profile of WS_2 nanosheets shows the step inside the WS_2 nanosheets with height different around 2-6 nm, as shown in **Fig. 4.** The exfoliation method which we choice in this content is possible to fold the WS_2 naosheets. We suggest that WS_2 nanosheets are folded and make the different of height inside the WS_2 nanosheets.

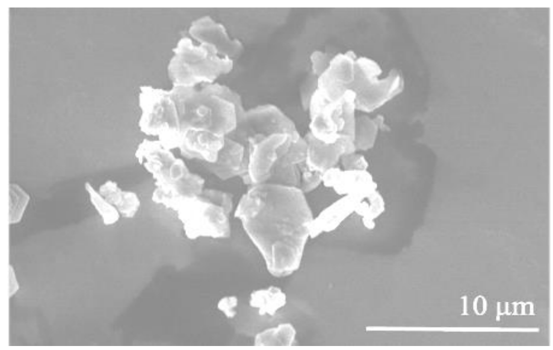

Fig. 2. Scanning electron microscopic images of bulk WS_2

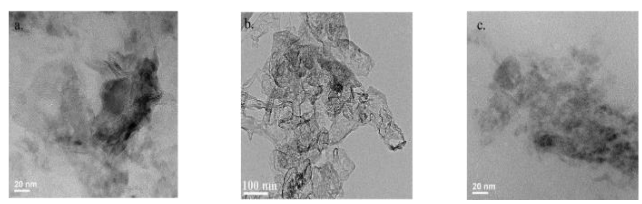

Fig. 3. Transmission electron microscopic images of WS_2 nanosheets from different concentration of n-butyllithium. (a) 0.33 M (b) 0.50 M (c) 0.67 M

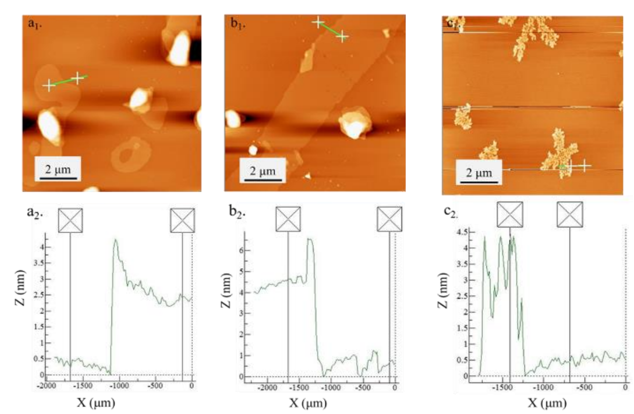

Fig. 4. Atomic Force Microscope image and height profile of WS_2 nanosheets from different concentration of n- butyllithium. (a1, a2) 0.33 M (b1, b2) 0.50 M (c1, c2) 0.67 M

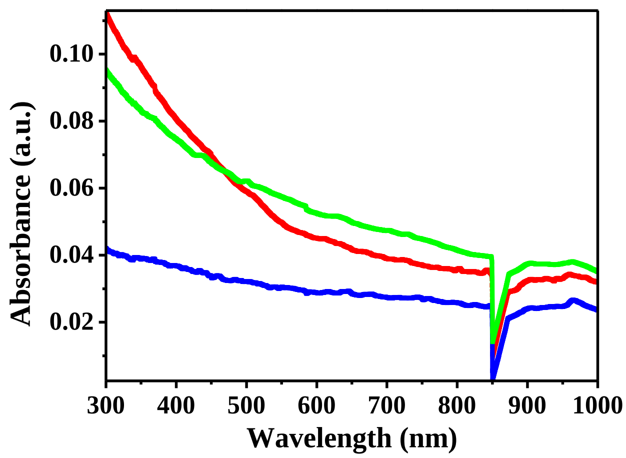

Fig. 5. UV-visible absorption spectra of WS_2 nanosheets from 0.33 M (red), 0.50 M (green) and 0.67 M (blue) of n-butyllithium.

Optical properties of WS_2 nanosheets

The **Fig. 5** is the UV-vis spectrum of WS_2 nanosheets prepared by three different concentration of n-butyllithium. The 2H-phase WS_2 shows mainly three peak around 630 to 650 nm, 550-500 nm and 450-500 nm [19,20]. However, spectrum shows that the absorbance of increase with decreasing wavelength and absent of the three characteristic peak of 2H-WS_2 which indicate that the WS_2 nanosheets are 1T phase.

Photoelectrochemical water splitting

The WS_2 nanosheets for photoelectrochemical water splitting were measured with electrolyte of 0.2 M $KHCO_3$ in DI-water : methanol = 1:1 solution under solar light radiation, as shown in **Fig. 6**. The efficiency was estimated according to following equation

$$\eta(\%)=\frac{(1.229-|Vbias|)\times I}{Pt}\times 100\%,$$

the efficiency of WS_2 is decreasing with increasing the concentration of n-butyllithium. The efficiency of WS_2 nanosheets decreases with the increasing n-butyllithium concentration. The WS_2 nanosheets prepared under the 0.33 M n-butyllithium solution show the highest efficiency among the other WS_2 nanosheets and the hydrogen generation rate is 4.81×10^{-4} L/s·m^2, as shown in **Table. 1**.

Table 1. Photoelectrochemical water splitting properties of WS_2 nanosheets under solar light radiation.

Parameters	J_{max} (A/m^2)	V_{max} (volt.)	η_{0max} (%)	$H_{2\,MAX}$ (L/s · m^2)
0.33 M	3.775	0.535	0.262	4.81×10^{-4}
0.50 M	3.169	0.532	0.221	4.04×10^{-4}
0.67 M	2.652	0.535	0.184	3.38×10^{-4}

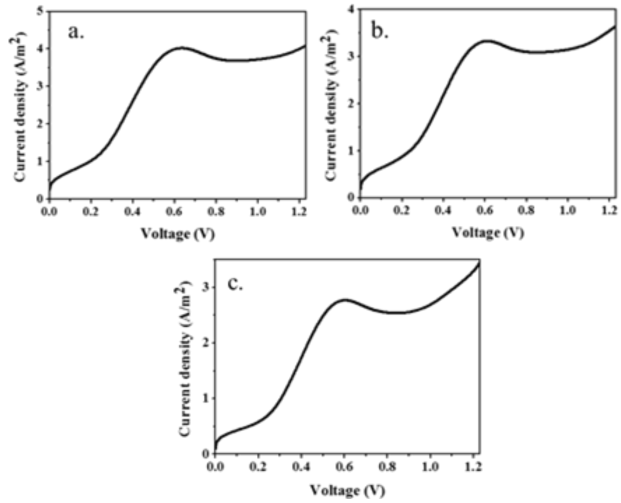

Fig. 6. J-V curve of WS_2 nanosheets from different concentration of n-butyllithium. (a) 0.33 M (b) 0.50 M (c) 0.67 M.

Conclusion

We have successfully prepared the few-layered 1T-WS_2 nanosheets by lithium intercalation in a teflon lined autoclave at a temperature of 100^{0}C for 5 hour. The lateral size of WS_2 nanosheets are about several hundred nanometers and the number of layer is about three to six layers. The highest efficiency of photoelectrical water splitting is at 0.535 voltage with current density = 3.775 A/m^2 and the hydrogen generation rate = 4.81×10^{-4} L/s · m^2. The few-layered 1T-WS_2 nanosheets show a good candidate for hydrogen evolution.

Acknowledgements

This work was financially supported by Ministry of Science and Technology of Taiwan and Academia Sinica, which is gratefully acknowledged

Supporting information

Supporting informations are available from VBRI Press.

References

1. Geim, A. K.; Novoselov, K. S; Nat. Mater., **2007**, 6(3), 183-191. **DOI:** 10.1038/nmat1849
2. Zhang, Y. B.; Tan, Y. W.; Stormer, H. L.; Kim, P; Nature, **2005**, 438(7065), 201-204. **DOI:** 10.1038/nature04235
3. Novoselov, K. S.; Geim, A. K.; Morozov, S. V.; Jiang, D.;. Katsnelson, M. I; Grigorieva, I. V.; Dubonos, S. V.; Firsov, A. A; Nature, **2005**, 438(7065), 197-200. **DOI:** 10.1038/nature04233
4. Eda, G.; Yamaguchi, H.; Voiry, D.; Fujita, T.; Chen, M. W.; Chhowalla, M; Nano Letters, **2011**, 11(12), 5111-5116. **DOI:** 10.1021/nl201874w
5. Lukowski, M. A.; Daniel, A. S.; Meng, F.; Forticaux, A.; Li, L. S.; Jin, S; Journal of the American Chemical Society, **2013**, 135(28), 10274-10277. **DOI:** 10.1021/ja404523s
6. Karunadasa, H. I.; Montalvo, E.; Sun, Y. J.; Majda, M.; Long, J. R.; Chang, C. J; Science, **2012**, 335(6069), 698-702. **DOI:** 10.1126/science.1215868
7. Merki, D.; Fierro, S.; Vrubel, H.; Hu, X. L; Chem. Sci., **2011**, 2(7), 1262-1267. **DOI:** 10.1039/c1sc00117e

8. Jaramillo, T. F.; Jorgensen, K. P.; Bonde, J.; Nielsen, J. H.; Horch, S.; Chorkendorff, I; Science, **2007**, 317(5834), 100-102.
DOI: 10.1126/science.1141483
9. Wang, H. T.; Lu, Z. Y.; Xu, S. C.; Kong, D. S.; Cha, J. J.; Zheng, G. Y.; Hsu, P. C.; Yan, K.; Bradshaw, V; Prinz, F. B.; Cui, Y; Proceedings of the National Academy of Sciences of the United States of America, **2013**, 110(49), 19701-19706.
DOI: 10.1073/pnas.1316792110
10. Lukowski, M. A.; Daniel, A. S.; English, C. R.; Meng, F.; Forticaux, A.; Hamers, R. J.; Jin, S; Energy Environ. Sci., **2014**, 7(8), 2608-2613.
DOI: 10.1039/c4ee01329h
11. Mahler, B.; Hoepfner, V.; Liao,V; Ozin, G. A; Journal of the American Chemical Society, **2014**, 136(40), 14121-14127.
DOI: 10.1021/ja506261t
12. Yang, D.; Frindt, R. F; J. Phys. Chem. Solids, **1996**, 57(6-8), 1113-1116.
DOI: 10.1016/0022-3697(95)00406-8
13. Pincella, F.; Isozaki, K.; Miki, K; Light-Science & Applications, **2014**, 3, 6.
DOI: 10.1038/lsa.2014.14
14. Voiry, D.; Yamaguchi, H.; Li, J. W.; Silva, R.; Alves, D. C. B.; Fujita, T.; Chen, M. W.; Asefa, T.; Shenoy, V. B. Eda, G. Chhowalla, M; Nat. Mater., **2013**, 12(9), 850-855.
DOI: 10.1038/nmat3700
15. Kung, P. Y.; Huang, L. W.; Shen, T. W.; Wang, W. L.; Su, Y. H.; Lin, M. I; Applied Physics Letters, **2015**, 106(2), 5.
DOI: 10.1063/1.4901944
16. Zeng, Z. Y.; Yin, Z. Y.; Huang, X.; Li, H.; He, Q. Y.; Boey, G. Lu, F.; Zhang, H; Angewandte Chemie-International Edition, **2011**, 50(47), 11093-11097.
DOI: 10.1002/anie.201106004
17. Yuwen, L. H.; Yu, H.; Yang, X. R.; Zhou, J. J.; Zhang, Q.; Zhang, Y. Q.; Luo, Z. M.; Su, S.; Wang, L. H; Chemical Communications, **2016**, 52(3), 529-532.
DOI: 10.1039/C5CC07301D
18. Ghorai, A.; Midya, A.; Maiti, R.; Ray, S. K;, Dalton Transactions, 2016, 45(38), 14979-14987.
DOI: 10.1039/C6DT02823C
19. Pagona, G.; Bittencourt, C.; Arenal, R.; Tagmatarchis, N; Chemical Communications, **2015**, 51(65), 12950-12953.
DOI: 10.1039/c5cc04689k
20. Atkin, P.; Daeneke, T.; Wang, Y.; Carey, B. J.; Berean, K. J.; Clark, R. M.; Ou, J. Z.; Trinchi, A.; Cole, I. S.; Kalantar-zadeh, K; Journal of Materials Chemistry A, **2016**, 4(35), 13563-13571.
DOI: 10.1039/C6TA06415A

SUPPORTING INFORMATION

a) The photoelectrical water splitting properties of PEDOT:PSS solution

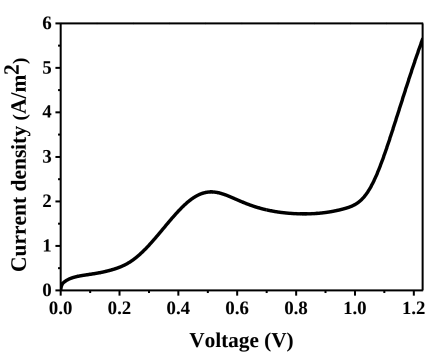

Fig. (a). The J-V curve of PEDOT:PSS solution
The highest efficiency is 0.1633% at 0.473 voltage with current density = 2.16 A/m^2 and hydrogen generation rate is 2.75 × 10^{-4} L/s·m^2